The influence of freeze–thaw cycles on the mechanical properties of paleosols: based on a multiscale research

Authors: Yiqian, Chen, Peiran, Zhang, Yang, Bai, Zihao, Zhou, Yongxin, Che, et al.

Source: Canadian Journal of Soil Science, 102(3) : 755-765

Published By: Canadian Science Publishing

URL: https://doi.org/10.1139/cjss-2021-0183

Canadian Journal of Soil Science

Article

The influence of freeze–thaw cycles on the mechanical properties of paleosols: based on a multiscale research

Chen Yiqian[a,b], **Zhang Peiran**[c], **Bai Yang**[a], **Zhou Zihao**[a], **Che Yongxin**[d], **and Yang Huimin**[a]

[a]School of Architecture and Civil Engineering, Xi'an University of Science and Technology, Xi'an, Shaanxi 710054, China; [b]Shaanxi Tiandi Geological Co., Ltd., Xi'an, Shaanxi 710054, China; [c]School of Civil Engineering, Central South University, Changsha, Hunan 410075, China; [d]Institute of New Energy and Low Carbon Technology, Sichuan University, Chengdu, Sichuan 610207, China

Corresponding author: **Chen Yiqian** (email: Chenyq96@163.com)

Abstract

To investigate the multiscale effects of freeze–thaw cycles on the mechanical properties and structural damage of paleosols, remodeled paleosol specimens at natural moisture content were subjected to multiple freeze–thaw cycles, followed by scanning electron microscopy, nuclear magnetic resonance (NMR) pore testing, and triaxial shear testing, and then the shear strength deterioration mechanism of paleosols was elaborated on from three aspects: fine, mesoscopic, and macroscopic. The main experimental results were as follows: (1) at the fine level, the NMR T_2 spectrum distribution curve showed one primary and two secondary peaks, in which the main spectrum occupied the majority, and the spectrum area showed an exponential function distribution relationship with the number of freeze–thaw cycles. With the accumulation of freeze–thaw cycles, the medium and large pores increased significantly. (2) At the mesoscopic level, when the specimens underwent freeze–thaw cycles, the interparticle contact pattern and particle morphology changed and the particle roundness increased. As the freeze–thaw cycle continued, fissures gradually developed and increased the most after the first freeze–thaw cycle, but the probability entropy of soil particles showed a decreasing trend with the increase of the number of freez–thaw cycles. (3) At the macro level, the number of freeze–thaw cycles gradually accumulated, the specimen stress–strain curve softened significantly, the shear strength deterioration effect was obvious, the deterioration value was the largest after one freeze–thaw cycle and gradually stabilized after 10 cycles, and the deterioration effect of cohesion was greater than that of the internal friction angle.

Key words: paleosol, freeze–thaw cycles, nuclear magnetic resonance, shear strength, deterioration mechanism

Résumé

Les auteurs souhaitaient approfondir l'effet du cycle gel-dégel sur les propriétés mécaniques des paléosols à diverses échelles ainsi que les dommages structuraux subis par ceux-ci. Dans cette optique, ils ont soumis les sols en question, remodelés à une teneur en eau normale, à une succession de cycles. Ensuite, ils les ont analysés par microscopie électronique à balayage, ont vérifié les pores par résonance magnétique nucléaire (RMN) et ont procédé à des essais de cisaillement triaxial avant d'élaborer le mécanisme de détérioration des paléosols attribuable à la force de cisaillement à trois échelles : fine, mésoscopique et macroscopique. Voici les principaux résultats de l'expérience. (1) Au niveau fin, la courbe de distribution du spectre RMN T_2 ne montre qu'un pic primaire et deux secondaires, où se retrouve la majeure partie du spectre. L'aire couverte par ce dernier est distribuée de façon exponentielle selon le nombre de cycles gel-dégel. Quand ce nombre augmente, on note une hausse importante des pores de taille moyenne ou de grande taille. (2) Au niveau mésoscopique, les cycles gel-dégel modifient la nature du contact entre particules et la morphologie des particules, qui s'arrondissent. Des fissures apparaissent peu à peu avec l'augmentation des cycles gel-dégel, les plus nombreuses survenant après le premier cycle. Toutefois, la probabilité de l'entropie des particules a tendance à diminuer à mesure que le nombre de cycles gel-dégel augmente. (3) Au niveau macroscopique, la courbe stress-contrainte du spécimen s'atténue nettement avec la hausse graduelle du nombre de cycles gel-dégel. La détérioration résultant de la force de cisaillement est manifeste. Elle atteint un maximum après le premier cycle avant de se stabiliser progressivement après le dixième. La cohésion se détériore plus que l'angle de friction interne. [Traduit par la Rédaction]

Mots-clés : paléosol, cycle gel-dégel, résonance magnétique nucléaire, force de cisaillement, mécanisme de dégradation

1. Introduction

As an important part of the loess stratum, paleosols are the product of soil deposition under wet and hot conditions, generally distributed in strips, usually as a carrier to reflect environmental changes. Paleosols are widely distributed in the northwest region of China, mostly in the seasonal frozen area, rainfall infiltration and repeated freezing and melting of the soil makes the paleosol itself structural changes,

making the area often cracked roadbed, slope failure and other phenomena, seriously endangering the safety of local residents and their property. Therefore, it is of great significance to investigate the engineering properties of paleosols under freeze–thaw cycles, especially the potential multiscale effects and mechanisms of their mechanical property degradation, for engineering construction and disaster prevention and control in paleosol regions.

For the study of paleosols, mechanically, Wang et al. (2021) have obtained the corresponding state unconfined compressive strength by an unconfined compressive strength test. Cao et al. (2016) have compared and analyzed the variability of shear damage forms of paleosols under consolidation undrained (CU) and consolidation drainage (CD) shear tests. Wu et al. (2019) have conducted triaxial shear tests on paleosols with different stress paths to clarify the soil deformation damage mechanism. Ye et al. (2019*a*,2019*b*) have explored the effects of the initial moisture content and wet and dry cycles on the mechanical properties of paleosols. Chang (2020) have tested the swelling rate of remodeled and in situ paleosols at different moisture contents, and the study showed that the swelling force of remodeled soil was greater than that of undisturbed soil when the moisture contents were the same. Ye et al. (2021*a*) have tested the swelling rate of paleosols in different states, and the results showed that the unloaded expansion rate of remolded soil was approximately twice that of undisturbed soil. Over the years, scholars in civil engineering have carried out a lot of research around the freeze–thaw properties of soils and have obtained many very constructive results, mainly in the areas of structural properties (Graham and Au 1985; Vikander 1998; Zhang et al. 2013), constitutive relations (Qi et al. 2006; Lai et al. 2010; Wang et al. 2010), microscopic properties (Lei et al. 2019; Xu et al. 2020), and shear strength (Han et al. 2018; Meeravali et al. 2020; Qin et al. 2021). However, the abovementioned studies mainly focus on shallow soils such as loess, expansive soils, and clay soils.

In the early 19th century, K. Terzaghi, a famous American geotechnical scientist, proposed the idea that "when studying the engineering properties of geotechnical bodies, attention should be paid to their microstructure," which has attracted the attention of geotechnical scholars. In the past century, with the development of science and technology, scanning electron microscopy (SEM), which is widely used in the field of chemical materials, and nuclear magnetic resonance (NMR), which is used in medicine, have gained a lot of applications and developments in geotechnical engineering, and many innovative research results have been achieved. Ahmadi et al. (2021) took a fine-grained soil from a seasonally frozen soil area as the research object, and explored the improvement effect of the low-carbon and environmentally friendly glass fiber on the strength characteristics of the fine-grained soil in the freezing and thawing environment, and used an electron microscope. The microstructure changes and interface interactions of fiber–clay particles have been analyzed. Firoozi et al. (2015) have explored the effect of freeze–thaw cycles on clay soils using electron microscopy and concluded that freeze–thaw cycles weaken the way in which soil particles are connected, thus causing a reduction in cohesion. In addition, electron microscopy has played an important role in studying the freeze–thaw mesoscopic properties of soils such as loess (Wang et al. 2021), chalky clay (Zhang et al. 2015), expansive soils (Zhao et al. 2021), and saline soils (Zhang et al. 2019). It is worth noting that NMR technology, which has the function of testing the T_2 relaxation time of rocks and soils to indirectly capture the pore distribution function, has received attention and application in the industry in recent years, especially in terms of rock freeze–thaw characteristics (Jia et al. 2020), measuring the T_2 spectrum of freeze–thaw sandstone by NMR and obtaining its pore evolution pattern. Tla et al. (2020) have used an NMR technique to study the mesoscopic damage mechanism of sandstones under freeze–thaw cycles. However, there are relatively few studies on NMR techniques for freeze–thaw soil testing.

In summary, most of the current studies on paleosols focus on general mechanical and swelling properties, and a few studies have been conducted on their freeze–thaw properties. In addition, for the characteristics of freeze–thaw soils, the current research methods are relatively mature; however, due to the more diverse freeze–thaw cycle test methods and research variables in the studies, the results vary greatly, and an especially comprehensive reflection of the fine–mesoscopic–macroscopic degradation mechanism under a freeze–thaw environment is rare, and it needs further exploration. In view of this, this paper took a paleosol (Q_3^{eol}) at the foot of a side slope in Yan'an, Shaanxi Province as the research object and subjected it to 0, 1, 4, 7, 10, and 15 freeze–thaw cycles, and then NMR, SEM, and triaxial shear tests were conducted to clarify the evolution law and inner correlation of the fine pore space, mesoscopic particles, and macroscopic strength of the soil, aiming to provide a reference for the engineering construction of a paleosol stratum in the monsoon freezing area.

2. Test soil sample and program

2.1. Test soil sample

The test soil sample was taken from the paleosol Q_3^{eol} (35°45′42″N, 109°27′41″E) at the foot of a slope in Yan'an, Shaanxi Province, showing yellow–brown color, containing some worm holes and a small amount of white calcareous nodules; the particle gradation curves are shown in Fig. 1 and the soil sample collection site is shown in Fig. 2*a*. According to the relevant provisions in the geotechnical test methods (GB/T50123-1999 (Chinese Standards)), indoor tests were conducted on it, and the basic physical properties of the soil samples were measured and are shown in Table 1.

2.2. Specimen preparation

In this test, unsaturated remodeled standard soil samples with $\varphi = 39.1$ mm and $h = 80.0$ mm were prepared under the condition of 95% compaction and natural moisture content (14.3%) (Fig. 2*b*). First, the retrieved soil samples were crushed and dried and passed through a 2 mm sieve. A fixed mass of fine-grained dry soil and purified water was weighed. The dry soil was divided into three equal masses

Fig. 1. Particle grading curve of paleosol.

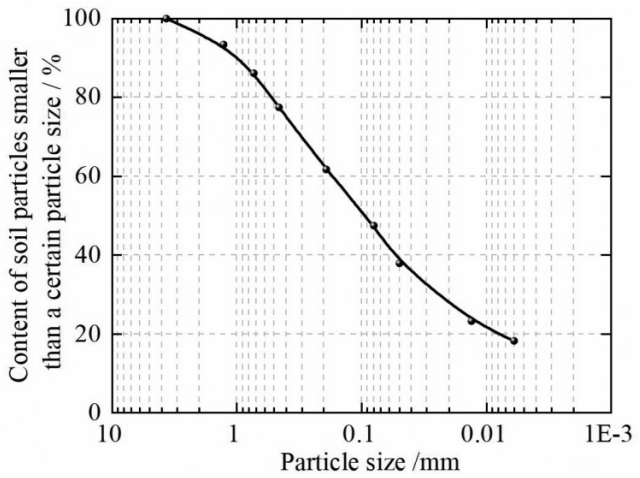

in the basin, and each layer of soil was sprayed with water immediately. After the layer of soil was spread, it was sealed and placed in a constant-temperature curing box for 24 h (Fig. 2*c*). After the curing was complete, it was compacted in five layers in the standard sample preparation instrument. To achieve homogeneity of the test soil samples, the dry density of the specimens was controlled to be 1.73 g·cm^{-3}, and the specimens were wrapped and sealed with cling film after preparation.

2.3. Experimental method

2.3.1. The freeze–thaw cycle test

Referring to the meteorological data of the fetching land, the lowest temperature in the area in the past 10 years is in January of each year, and it is −21.8 °C, and the average temperature is −14.3 °C, so the freezing temperature of the test design was −15 °C, and regarding the choice of melting temperature, some studies showed that the influence of melting temperature on the mechanical characteristics of the soil is negligible (Kamei et al. 2012), and to simplify the melting conditions of the soil, the melting temperature was set to 25 °C. To simulate the diurnal temperature rise and fall pattern, the freezing temperature was slowly increased to the melting temperature. Reference to other scholars' research, (Zhang et al. 2013; Chang et al. 2014; Liu et al. 2016), the soil strength decay effect is most obvious after 1 freeze–thaw cycle, fluctuates 6–8 times more, and can basically reach a new stable state after about 10 times, so the number of freeze–thaw cycles was 0, 1, 4, 7, 10, and 15, for a total of 6. The freeze–thaw test was conducted in a special test chamber with a temperature control range of –40 °C∼+120 °C and an accuracy of ±0.1 °C. The freeze–thaw test could meet the requirements of this freeze–thaw cycle test (Fig. 2*d*). To simulate the natural diurnal freeze–thaw cycle duration, the freezing and thawing duration were set to 12 h, and this process was a freeze–thaw cycle.

2.3.2. Nuclear magnetic resonance test

Nuclear magnetic resonance technology is used to study the nuclear spin in a low-energy state to absorb the energy provided by the radio frequency field to transition to a high-energy state and use the energy change of the nucleus in a magnetic field to obtain information about the nucleus. It is known from the basic theory of NMR that when the porous medium is completely saturated with water, the T_2 value of a single pore is proportional to the ratio of the pore surface area to the volume, so the pore size distribution characteristics of the soil sample are converted from the observed T_2 distribution of all pores. The expression for the relaxation time T_2 of the soil material is as follows:

$$(1)\quad \frac{1}{T_2} = \frac{S}{T_{2(\text{free})}} + \frac{S}{T_{2(\text{surface})}} + \frac{S}{T_{2(\text{diffusion})}}$$

$$(2)\quad \frac{1}{T_2} = \frac{S}{T_{2(\text{free})}} + \rho_2\left(\frac{S}{V}\right)_{\text{pore}} + \frac{D(\gamma G T_E)^2}{12}$$

Here, $T_{2\,(\text{free})}$ is the free relaxation time of the fluid, which is determined by the physical properties of the fluid; $T_{2\,(\text{surface})}$ is the surface relaxation time of the fluid, obtained from the ratio of the surface relaxation strength (ρ_2) and pore surface area to fluid volume; and $T_{2\,(\text{diffusion})}$ is the diffusion relaxation time of the fluid, calculated from the diffusion coefficient (D), the magnetic field strength (G), the magnetic spin ratio (γ), and the sequence parameter (T_E) at the time of measurement.

In the calculation, $T_{2\,(\text{free})}$ and $T_{2\,(\text{diffusion})}$ are neglected, and the relaxation time is mainly determined by $T_{2\,(\text{surface})}$. Simplifying eq. 2 yields

$$(3)\quad \frac{1}{T_2} = \rho_2\left(\frac{S}{V}\right)_{\text{pore}}$$

Here, ρ_2 is the transverse relaxation rate and S/V is the ratio of surface area to volume of water-filled pores in the soil sample.

When the soil sample reached the number of freeze–thaw cycles, a saturation instrument was used to vacuum the sample after the cycle (Fig. 2*e*), and it was put into the saturation instrument to saturate for 12 h after completion so that the soil saturation was more than 98%. After the end, NMR was carried out for detection, and the other group was not saturated for triaxial shear test. The instrument used in this experiment was the C12-010V NMR analyzer (Fig. 2*f*). The remodeled soil samples that had undergone different freeze–thaw cycles were measured, and the pore size distribution of the soil samples caused by the freeze–thaw cycles was analyzed.

2.3.3. Scanning electron microscopy scan test

When the freeze–thaw cycle was completed, the specimens were dried, cut, and gold sprayed (Fig. 2*g*), and for each

Fig. 2. Test procedure and apparatus. (*a*) The soil sample collection site, (*b*) unsaturated remodeled standard soil samples, (*c*) constant-temperature curing box, (*d*) temperature control box, (*e*) saturation instrument, (*f*) C12-010V NMR analyzer, (*g*) sample drying and gold spraying device, (*h*) HITACHI SU6600 scanning electron microscope equipment, (*i*) strain-controlled fully automatic triaxial instrument, (*j*) pressure chamber. [Color online]

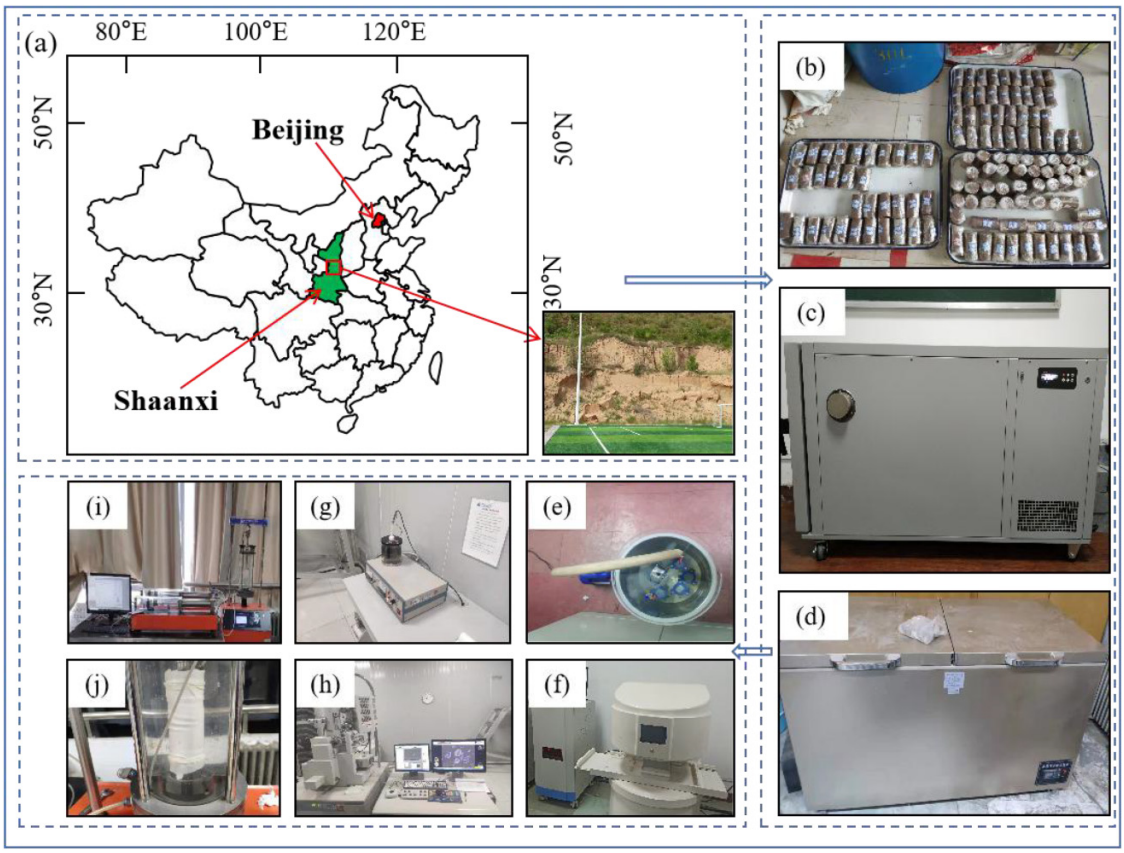

Table 1. Basic physical properties of soils.

Moisture content (W; %)	Dry density (ρ; gcm^{-3})	Maximum dry density ($_{dmax}$; gcm^{-3})	Specific gravity (G_S)	Liquid limit (W_L; %)	Plastic limit (W_P; %)
14.3	2.23	1.82	2.70	43.17	26.55

scanned soil sample, representative scanning points were selected to be photographed. The test was carried out with HITACHI SU6600 scanning electron microscope equipment (Fig. 2*h*) under a high-vacuum scanning environment, and at the same time, different magnifications were used to observe and photograph to obtain more information about the soil microstructure, and finally the SEM images with the most abundant image information were selected. The acquired SEM images were processed and analyzed with PCAS software (Liu et al. 2011, 2013), which identifies the mesoscopic images and then segments the fine connections between the pores by erosion operations to obtain the real pores between the particles, and colorized identification. Then, the geometric and statistical parameters of the mesoscopic images were quantitatively outputted, the geometric parameters including the fissure length and area and the statistical parameters including the particle circularity and probability entropy. The software is in pixels and the formula is given in eqs. 4 and 5. SEM images are shown in Fig. 3*a*. The SEM image was denoised to obtain the binary image including soil particles and pores, and is different from the original SEM image, and the pores and soil particles could be separated for the next step of processing; binary maps are shown in Fig. 3*b*. Through the further processing of the binary image, the pores were colored with different colors to quantify the pore parameters, and the image after color recognition is shown in Fig. 3*c*.

$$S_t = \frac{S}{R^2} \quad (4)$$

$$C_t = \frac{C}{R^2} \quad (5)$$

Here, R is the SEM image resolution, S a nd$C$ are the pixel area and pixel perimeter, respectively, and S_t and C_t are the real area and real perimeter, respectively.

Fig. 3. Mesoscopic image recognition. (*a*) Scanning electron microscopy image, (*b*) binary diagrams, and (*c*) colorized identification. [Color online]

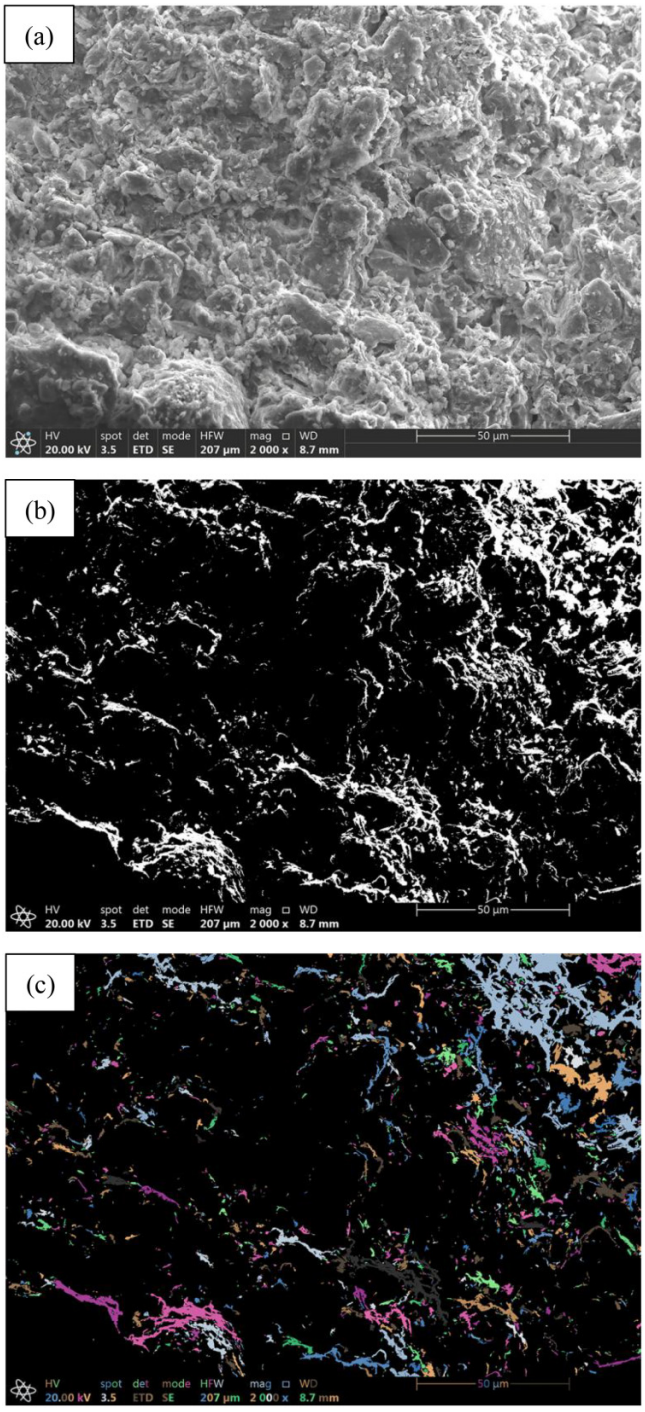

2.3.4. Triaxial shear test

The CU shear test was conducted when the number of freeze–thaw cycles reached the test design value. The test confining pressure was selected to be 50, 100, 200, and 400 kPa. The test was conducted on a strain-controlled fully automatic triaxial instrument (Figs. 2*i* and 2*j*), and the axial loading rate was set to 0.5% per minute.

3. Experimental results and analysis

3.1. Fine level — NMR pore test

To investigate the distribution of the fine pore evolution of paleosols after the different numbers of freeze–thaw cycles, NMR tests were conducted on the specimens after the freeze–thaw cycles, and the T_2 spectrum and pore change curve under the NMR test are shown in Fig. 4. The NMR signal is dimensionless and is automatically generated by the test instrument.

Analysis of Fig. 4*a* shows that, in general, in the distribution of the T_2 spectra of paleosols under the different numbers of freeze–thaw cycles there are one main peak and two secondary peaks, and the main peak is much larger than the two secondary peaks, which also reflects that the distribution of pores is mainly reflected in the distribution of the main peak when the specimens are subjected to different numbers of freeze–thaw cycles. Although the number of freeze–thaw cycles was different, the distribution intervals of the main peaks are all concentrated between 0.15 and 1.5. When the specimens did not experience freeze–thaw cycles, the peak T_2 spectra were the lowest, and with the freeze–thaw cycles, the peak T_2 spectra showed a gradual increase. Observing the local details, it can be seen that after experiencing one freeze–thaw cycle, the main peak of the T_2 spectrum appears to increase significantly, and the increase becomes smaller and smaller when the number of freeze–thaw cycles gradually increases. According to the NMR theory, the transverse relaxation time T_2 distribution reflects the pore size information, and the smaller is the T_2 value, the smaller is the pore size represented, and conversely the larger is the pore, the larger is the T_2 value. Meanwhile, the variation of the relaxation time and nuclear magnetic signal integration area can reflect the variation of the total pore volume within the soil. Based on this, it can be inferred that under the first freeze–thaw cycle, the pore volume appears to increase significantly, and then, while it still increases, the increased amount gradually decreases and stabilizes at 10 freeze–thaw cycles.

Figure 4*b* shows the change trend curve of the spectrum area of the paleosol samples corresponding to different freeze–thaw cycles, which also indirectly reflects the change of the pore volume in the soil with the number of cycles. With the freeze–thaw cycles, the spectral area shows an overall trend of increasing. When one freeze–thaw cycle is carried out, the spectral area changes the most, so it can be considered that the initial freeze–thaw cycle has the greatest effect on the pore volume; as the freeze–thaw alternation proceeds, more and more pores are formed between the soils, and more water seepage channels are formed, which makes the water migration process smoother, and the spectral area changes gradually decrease at this time. The results form a good correspondence with the inversion process in Fig. 4*a*, and there is a good functional relationship between the spectral area and the number of freeze–thaw cycles.

The biggest advantage of the NMR T_2 spectrum test is that it can quantitatively test the pores under nondestructive conditions. According to the existing research results (Ye et al. 2021*b*), the pores in the soil body can be classified

Fig. 4. The T_2 spectrum and pore change curve under the nuclear magnetic resonance test. (*a*) Nuclear magnetic signal curves under different freeze–thaw times, (*b*) trend of T_2 spectrum area under freeze–thaw cycles, and (*c*) variation of pore ratio at different scales in relation to the number of freeze–thaw cycles. [Color online]

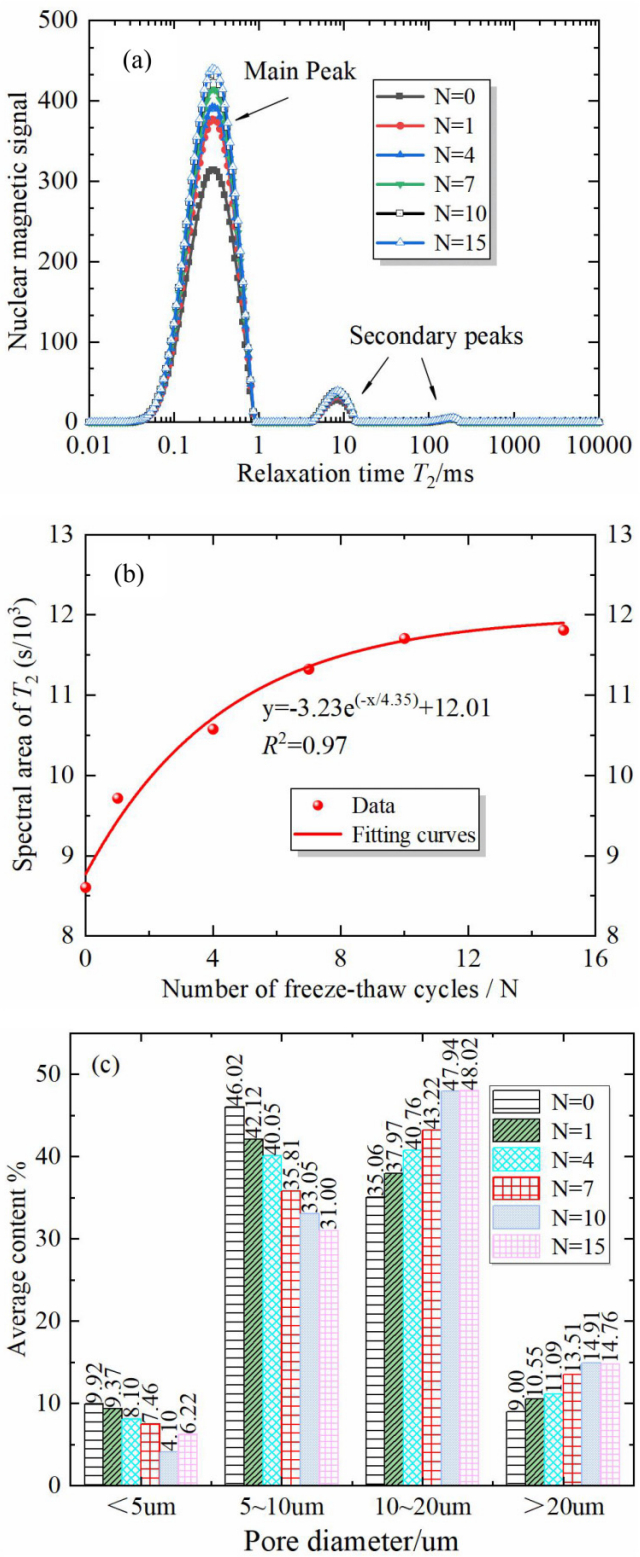

into four different types according to their size: micropores, $D < 5$ μm; small pores, 5 μm $\leq D <$ 10 μm; medium pores, 10 μm $\leq D <$ 20 μm; and large pores, 20 μm $\leq D$. According to the principle of NMR, combined with eq. 3, considering the structural characteristics of the soil sample itself, the surface relaxation strength $\rho_2 = 3.0$ μm·ms^{-1} was taken, and assuming that the pores in the soil sample are ideally spherical, $(S/V)_{pore} = 3/r$. By further transforming eq. 3, the relationship between the pore size in the soil and its internal pore water relaxation time T_2 can be obtained in the following equation (Wu et al. 2019):

$$\frac{1}{T_2} = \rho_2 \left(\frac{S}{V}\right)_{pore} \approx \rho_2 \frac{3}{r} \quad (6)$$

$$r = 9T_2 \quad (7)$$

Here, r is the pore radius.

According to eq. 7 and Figs. 4 and 5, the relationship between the changes of different sizes of pores of the specimen after experiencing different numbers of freeze–thaw cycles can be calculated.

Analysis of Fig. 4*c* shows that with the increase of the number of freeze–thaw cycles, the percentage of micro- and small pores in the soil gradually decreases, by 3.6% and 15.1%, and the percentage of medium and large pores gradually increases, by 12.9% and 5.8%, during the whole freeze–thaw process. In the process of repeated freezing and thawing of the specimen, along with the migration of water and phase change, resulting in the gradual dissolution of the adhesive colloid around the particles to produce relative displacement of tiny particles, when the number of freezing and thawing cycles gradually accumulates, on the one hand, the reciprocation of water causes the continuous dissolution of interparticle cementing material, leading to the evolution of some micro- and small pores into medium and large pores by connecting and developing, and on the other hand, when the soil melts, after the ice crystals liquefy into water, they migrate back under the action of temperature and part of the free water dissipates in the form of water vapor, and the pores are gradually released. Due to the large volume of ice crystals, the soil melts and the spacing of the filled particles exceeds the range of the adhesive force of the cementing substance, thus causing irrecoverable medium and large pores.

3.2. Mesoscopic-level SEM morphology test

3.2.1. Qualitative study of mesoscopic images

To qualitatively describe the change state of the mesoscopic image of the soil after a freeze–thaw cycle, it was necessary not only to ensure that the mesoscopic image was clear enough, but also to meet the rich information of pores and particles in the field of view. Due to the limitation of space, only the mesoscopic images after 0, 7, and 15 freeze–thaw cycles are given in this paper in Fig. 5.

From Fig. 5*a*, it can be seen that when the soil sample has not experienced freeze–thaw cycles, the soil particles are

Fig. 5. Scanning electron microscopy images with different numbers of freeze–thaw cycles. (*a*) $N = 0$, (*b*) $N = 7$, and (*c*) $N = 15$.

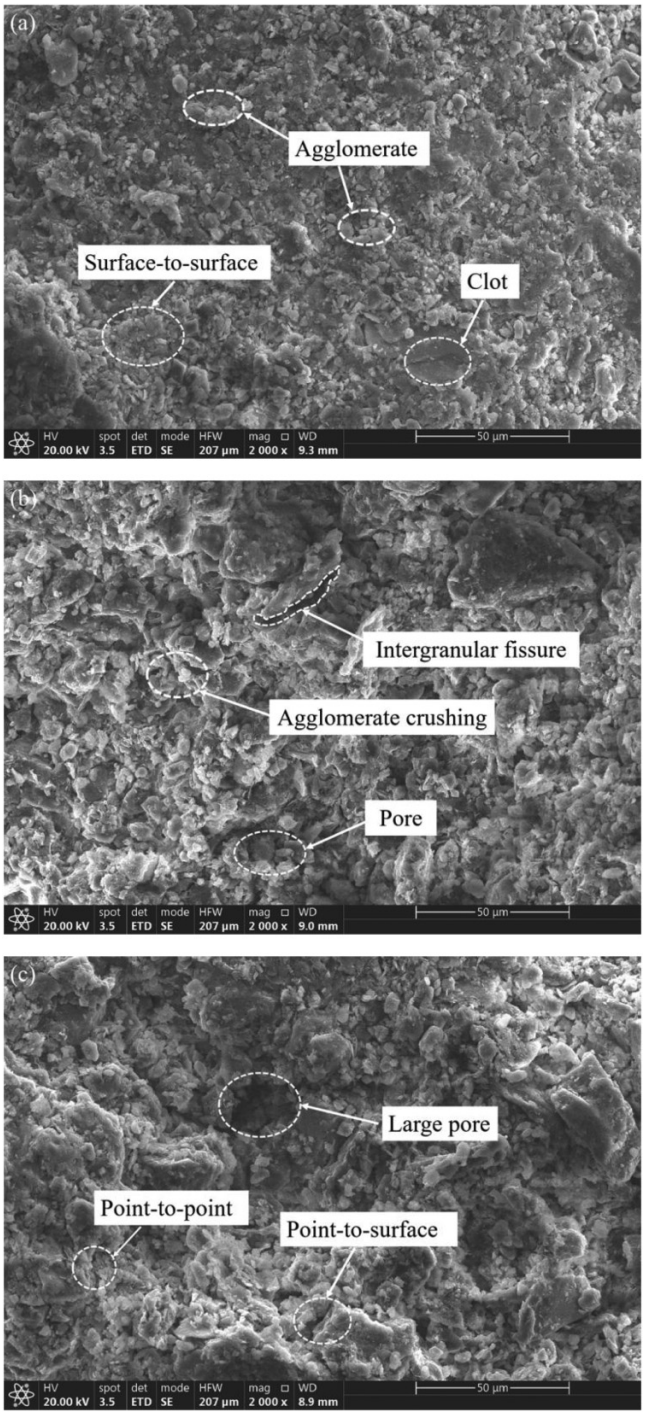

densely arranged, the structure type is mainly flocculent and agglomerated, the soil particles are mostly agglomerated and clotted, among which many small particles were attached to a large particle, the contact between particles is mainly in the form of face-to-face contact, and the pore type is mainly small pores. When the freeze–thaw cycles gradually accumulate, the soil particle skeleton and pore morphology change significantly, the agglomeration between the particles is destroyed, some of the particles begin to separate and gradually fall off, and they are scattered around other particles and in the pores, as shown in Fig. 5*b*, so the pore shape in the soil is constantly changing, the pores are developed, and the cracks are connected. The reason for the abovementioned phenomenon is as follows: due to the existence of free water in the sample, when the soil is frozen, the free water in the pores of the soil condenses into ice to form a cold structure. Since the volume of ice is greater than the volume of water, with the expansion force generated on the surrounding particles extrusion occurs; when the soil melts, the ice crystals filled in the pores melt into water and gradually dissipate, but the soil particle skeleton cannot be completely restored to the original state, resulting in continuous accumulation of pores, which is manifested by an increase in the number of pores in the soil and an increase in pore space, with the structure tending to be loose. At this time, the point-to-surface contact and point-to-point contact between particles are obvious, as shown in Fig. 5*c*.

3.2.2. Circularity of particles

Figure 6*a* shows the variation of the average circularity of the particles versus the number of freeze–thaw cycles obtained after processing on the mesoscopic images of the specimens.

Generally speaking, the average circularity of the particles tends to increase with the number of freeze–thaw cycles, which is mainly due to the dispersion of the complex-shaped agglomerates into small round particles by the freeze–thaw cycles. In addition, it is worth noting that the average circularity of the particles is in the rapid growth stage during the first freeze–thaw cycle, and then the growth of the roundness of the particles tends to slow down with the increase of the number of freeze–thaw cycles, which is mainly because the soil structure is good when the specimen is not frozen and thawed initially. When freezing and thawing occur, the original structure of the soil is rapidly destroyed under the action of the frost heave force, and the elongated particles tend to be squeezed by the ice crystals and gradually disintegrate to a round transition.

Figure 6*b* shows the relationship between the average length of fracture and the average area of pore space of the specimens with the number of freeze–thaw cycles. As shown in the figure, both curves show exponential variation with the number of freeze–thaw cycles, and the overall first increases and then basically stabilizes. Taking the average length of the cracks as an example, after the first freeze–thaw cycle, the average length of the cracks increased by 69.38 μm, an increase of 27.3% of the total. After 10 freeze–thaw cycles, the average length of the cracks only increased by 23.6 μm, accounting for 8.5%; when the freezing and thawing were complete, the increase was very small, only 3.2%. The reason for the abovementioned phenomenon is that the first freeze–thaw cycle applies a freeze–dilatation force (freeze–thaw tension) on the basis of the original equilibrium state of the soil, forcing the soil particles to change their morphology and contact mode, which is quantitatively expressed as an increase

Fig. 6. Mesoscopic particles and fracture variation curves under a scanning electron microscope. (*a*) Variation curve of particle circularity with the number of freeze–thaw cycles, (*b*) relationships between the average length of fracture and the average area of pore space of specimens with the number of freeze–thaw cycles, and (*c*) variation curve of probability entropy of soil particles with the number of freeze–thaw cycles. [Color online]

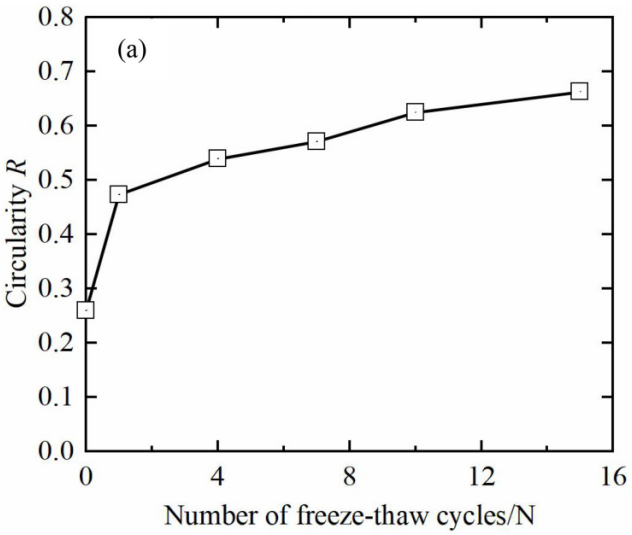

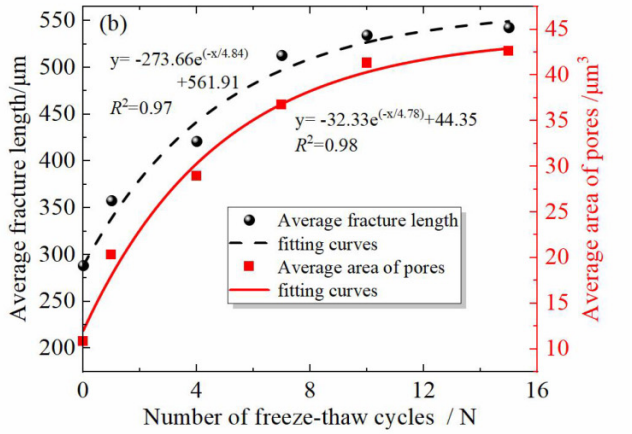

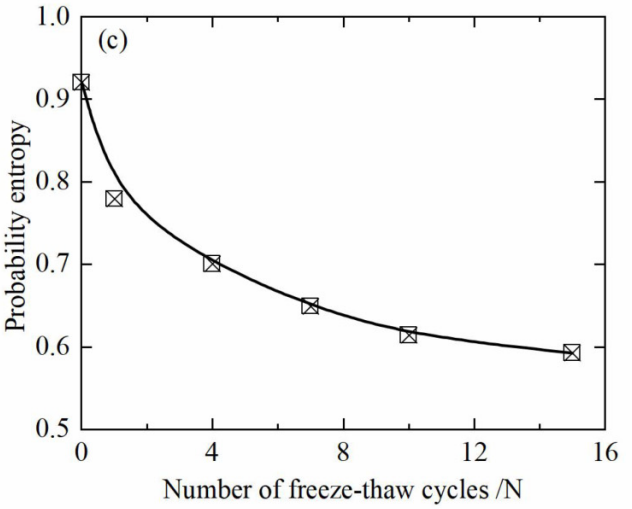

in the proportion of round-like particles (increase in circularity). Due to the small contact surface between round particles and the appearance of indirect contacts such as point–point contact and point–surface contact (mentioned before), pores are more likely to form around the granular body, and when the proportion of medium and large pores in the soil increases, they penetrate into the native fine cracks and microvoids, which then evolve into long cracks, thus causing the pore area to increase with the increase of the number of freeze–thaw cycles. When the proportion of medium and large pores in the soil increases, they intersect with the original fine cracks and microvoids, and then evolve into long cracks, causing the pore area to increase with the increase in the number of freeze–thaw cycles. When the freeze–thaw cycle reaches 10, both the average length of fissure and the average area of the pore change curve tend to level off, which is because the specimen has been fatigue damaged under the effect of freeze–thaw and the simple freezing–expansion force can no longer cause a large impact, or in the process of generating new fissures, some soil particles are squeezed and produce relative displacement, causing some primary or associated fissures to recover, so the development of cracks in the mesoscopic system of soil particles reaches a dynamic equilibrium.

Probability entropy is a structural parameter describing the particle arrangement, which can be used to analyze the soil particle arrangement after the freeze–thaw cycles. As shown in Fig. 6*c*, the probability entropy of the specimens gradually decreases with the increase of the number of freeze–thaw cycles, which indicates that the freeze–thaw action has a certain influence on the orientation of the soil particle arrangement, where the slope of the probability entropy change curve of the specimens under the first freeze–thaw cycle is the largest, indicating that the soil particle arrangement is the most sensitive to the first freeze–thaw cycle. According to the definition of probability entropy, under the action of freezing and thawing, the particle arrangement develops from a chaotic state to an orderly state; that is, the directionality of the particle arrangement gets better and better, which is also consistent with the development law of the circularity of the soil particles above. Correspondingly, with the change of the number of freeze–thaw cycles, soil particles gradually evolve and develop to round and near-circular shapes, which is quantitatively expressed as the smaller probability entropy of soil particles.

3.3. Macroscopic-level mechanical properties and strength parameter study

3.3.1. Stress–strain curve

The test soil samples were subjected to freeze–thaw cycles according to the scheme described in the Experimental methods section (eq. 1), followed by triaxial shear tests according to eq. 4 in the same section, and some representative stress–strain curves were selected. For the specimens with the curve form of strain-softening type, the value of partial stress at the peak point of the curve was taken as the shear strength; for the specimens with strain-hardening type, the value of partial

stress corresponding to 15% of the axial strain was taken as the shear strength. According to the Mohr–Coulomb strength criterion, the shear strength of the specimens after freeze–thaw cycles and the corresponding strength parameters were obtained. Shear strength and strength parameter variation curves are shown in Fig. 7.

As shown in Fig. 7*a*, the stress–strain curves of the specimens under different confining pressures are of strain-softening type, and the degree of strain softening gradually decreases with the decrease of the confining pressure, and the damage form is transformed from brittle damage to plastic damage. As shown in Fig. 7*b*, the peak stress decayed significantly with the increase of the number of freeze–thaw cycles under the circumferential pressure of 400 kPa, and was the most intense during the first freeze–thaw cycle, after which the degree of influence gradually weakened with the increase of the number of freeze–thaw cycles. Taken together, the greater is the number of freeze–thaw cycles at the same confining pressure level, the greater is the softening of the curve peak stress and the smaller is the value of partial stress required to produce the same axial strain; that is, there is a significant deterioration effect on the macroscopic shear strength of the soil.

3.3.2. Shear strength and corresponding parameters

From Fig. 7*c*, a significant deterioration effect of shear strength of the specimens was observed with the increase of the number of freeze–thaw cycles, but the performance varied at different confining pressures; specifically, the deterioration effect of shear strength increased with the increase of the confining pressure. Under four groups of confining pressure, the degradation of shear strength was the most serious after the first freeze–thaw cycle, and the loss values accounted for 37.1%, 32.5%, 30.4%, and 29.8% of the loss values during the whole freeze–thaw cycle, after which the degradation of shear strength gradually decreased with the increase of the number of freeze–thaw cycles, and the values of shear strength basically approaches at the 10th and 15th freeze–thaw cycles.

The relationship between the strength parameters and the number of freeze–thaw cycles in Fig. 7*d* shows that, in general, the cohesion and shear strength of the specimens are consistent; that is, they both decay with the increase of the number of freeze–thaw cycles, but the degrees of decay are different. The degree of cohesion deterioration is divided into three stages: the acute deterioration stage (0–1 times), indicating that the first freeze–thaw cycle has the greatest impact on the soil strength, and the cohesion at this stage decreases from the initial value of 67.06 to 53.28 kPa, accounting for 44.7% of the entire freeze–thaw process, the slow deterioration stage (1–10 times), where the cohesion is still decreasing, but the decrease is significantly smaller than that of the equilibrium stage (10–15 times), in which the cohesive force of the soil no longer changes with the number of freeze–thaw cycles, indicating that the mechanical behavior of the soil has reached a new equilibrium state, and the freeze–thaw

Fig. 7. Shear strength and strength parameter variation curves. (*a*) Effect of confining pressure, (*b*) effect of the number of freeze–thaw cycles ($\sigma_3 = 400$ kPa), (*c*) shear strength, and (*d*) strength parameters. [Color online]

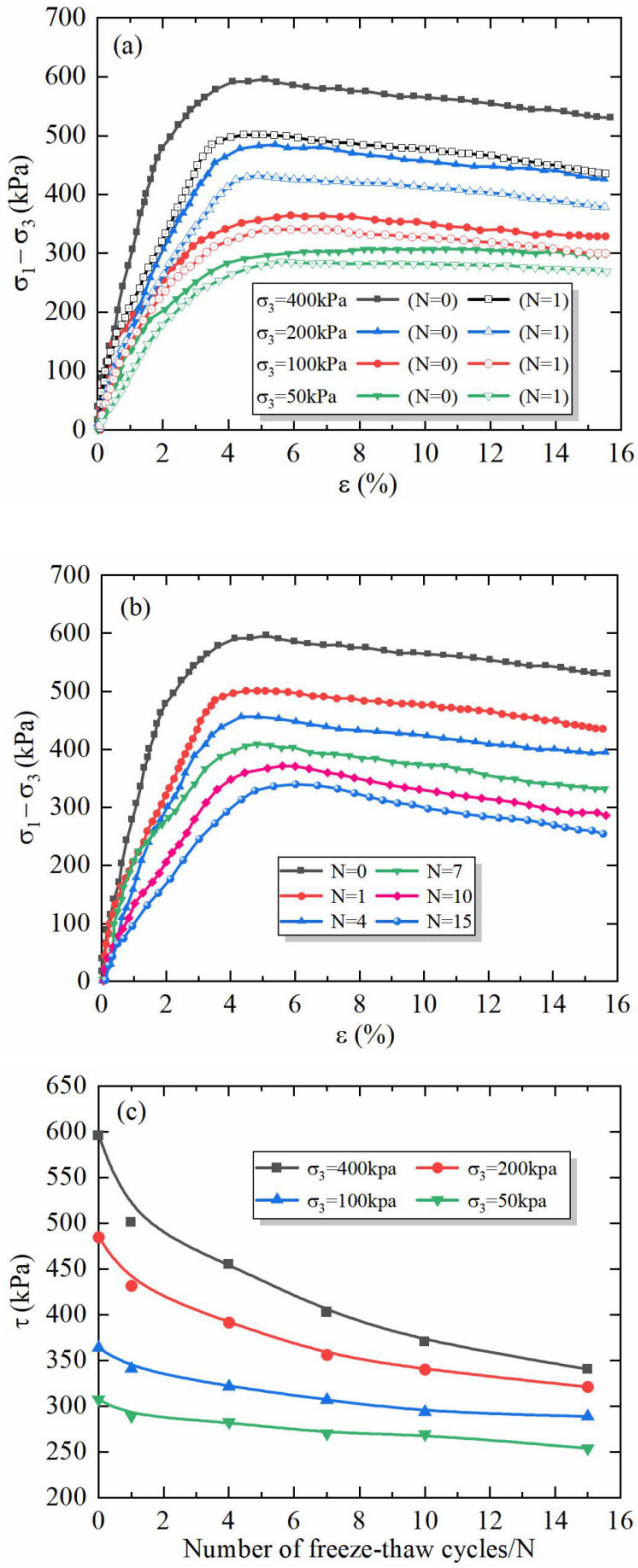

action no longer has an effect on the equilibrium state or has little effect and cannot break the equilibrium state. Although the angle of internal friction fluctuates with the number of freeze–thaw cycles, it still shows a decreasing law of change, but the magnitude is very small and far lower than the degradation of cohesion. It is also evident that for paleosols, the most important cause of degradation damage in shear strength after experiencing freeze–thaw is the decay of cohesion. For clay soils, cohesion is mainly controlled by the contact state between soil particles, and according to the experimental results obtained above (Section 3.2), with the change in the number of freeze–thaw cycles, the transformation of the contact mode between soil particles causes a weakening of the friction between the particles, which in turn causes a decrease in the angle of internal friction. In summary, under the freeze–thaw environment, the contact state of soil particles and the change of cementation cause the change of cohesion and internal friction angle, which in turn leads to the reduction of soil shear strength under the combined effect of both. However, in general, the decay of cohesion is the most important cause of shear strength deterioration.

4. Conclusion

(1) Under the action of freeze–thaw cycles, the T_2 spectrum distribution curve of the soil showed a typical distribution of one main peak and two secondary peaks, in which the main spectrum occupied the majority, being mainly concentrated in the range of 0.15∼1.5 ms, and the T_2 spectrum area change curve with the change of the number of freeze–thaw cycles, which showed a faster increasing trend and then gradually tended to level off. With the increase of the number of freeze–thaw cycles, the micro- and small pores of the specimen gradually developed through to the medium and large pores.

(2) Under the action of repeated freeze–thaw cycles, the microstructure of the soil changed significantly, and the particle contact changed from stable contact of surface–surface and edge–surface to unstable contact forms such as point–surface and point–point. With the increase of the number of freeze–thaw cycles, the roundness of the particles in the specimen increased, and the average length of the fissure and the average area of the pore increased, and the increase was the largest after the first freeze–thaw cycle, and after 10 freeze–thaw cycles, the two change curves tended to level off, and the particle probability entropy gradually decreased with the increase of freeze–thaw cycles, which indicates that the orientation of soil particles was getting better.

(3) The mechanical properties and shear strength of the soil under the freeze–thaw environment showed different degrees of deterioration effects, including significant softening of the stress–strain curve, dramatic loss of shear strength, exponential trend decay of cohesion, and the largest loss value during the initial freeze–thaw period, with a loss of 44.7%, and the internal friction angle always showed small, irregular fluctuations but the overall trend of reduction.

Article information

History dates

Received: 30 November 2021
Accepted: 7 March 2022
Version of record online: 2 September 2022

Notes

This paper is part of a Collection entitled “Soil Health Evaluation: Methods and Directions”.

Data availability

Some or all of the data used during the study are available from the corresponding author by request.

Author information

Competing interests

The authors declare no conflict of interest.

Funding information

This research was supported by the National Natural Science Foundation of China (grant no. 51778641).

References

Ahmadi, S., Ghasemzadeh, H., and Changizi, F. 2021. Effects of a low-carbon emission additive on mechanical properties of fine-grained soil under freeze–thaw cycles. J. Cleaner Prod. **304**(4): 127157. doi:10.1016/j.jclepro.2021.127157.

Cao, C.S., Wu, S.R., Pan, M., et al. 2016. Mechanics characteristics of paleosol and its implication to loess landslide. Hydrogeol. Eng. Geol. **43**(5): 127–131.

Chang, D., Liu, J.k., Li, X., and Yu, Q.M. 2014. Experiment study of effects of freezing–thawing cycles on mechanical properties of Qinghai–Tibet silty sand. Chin. J. Rock Mech. Eng. **33**(7): 1496–1502.

Chang, S.B. 2020. Influence of water content on swelling of surrounding rock of paleosol tunnel. Railw. Eng. **60**(6): 60–66.

Firoozi, A.A., Taha, M.R., Firoozi, A.A., and Khan, T.A. 2015. The influence of freeze–thaw cycles on unconfined compressive strength of clay soils treated with lime. J. Teknol. **76**(1): 107–113. doi:10.11113/jt.v76.4127.

Graham, J., and Au, V.C.S. 1985. Effects of freeze–thaw and softening on a natural clay at low stresses. Can. Geotech. J. **22**(1): 69–78. doi:10.1139/t85-007.

Han, Y., Wang, Q., Wang, N., Wang, J., Zhang, X., Cheng, S., and Kong, Y. 2018. Effect of freeze–thaw cycles on shear strength of saline soil. Cold Reg. Sci. Technol. **154**: 42–53. doi:10.1016/j.coldregions.2018.06.002.

Jia, H., Ding, S., Zi, F., Dong, Y., and Shen, Y. 2020. Evolution in sandstone pore structures with freeze–thaw cycling and interpretation of damage mechanisms in saturated porous rocks. Catena, **195**: 104915. doi:10.1016/j.catena.2020.104915.

Kamei, T., Ahmed, A., and Shibi, T. 2012. Effect of freeze–thaw cycles on durability and strength of very soft clay soil stabilised with recycled bassanite. Cold Reg. Sci. Technol. **82**(8): 124–129. doi:10.1016/j.coldregions.2012.05.016.

Lai, Y., Yang, Y., Chang, X., and Li, S. 2010. Strength criterion and elasto-plastic constitutive model of frozen silt in generalized plastic mechanics. Int. J. Plast. **26**(10), 1461–1484.

Lei, H., Song, Y., Qi, Z., Liu, J., and Liu, X. 2019. Accumulative plastic strain behaviors and microscopic structural characters of artificially freeze–thaw soft clay under dynamic cyclic loading. Cold Reg. Sci. Technol. **168**: 102895. doi:10.1016/j.coldregions.2019.102895.

Liu, C., Shi, B., Zhou, J., and Tang, C. 2011. Quantification and characterization of microporosity by image processing, geometric measurement and statistical methods: application on sem images of clay materials. Appl. Clay Sci. **54**(1): 97–106. doi:10.1016/j.clay.2011.07.022.

Liu, C., Tang, C.S., Shi, B., and Suo, W.B. 2013. Automatic quantification of crack patterns by image processing. Comput. Geosci. **57**(4): 77–80.

Liu, J.K., Chang, D., and Yu, Q.M. 2016. Influence of freeze–thaw cycles on mechanical properties of a silty sand. Eng. Geol. **210**(5): 23–32. doi:10.1016/j.enggeo.2016.05.019.

Meeravali, K., Alla, S., Syed, H., and Ruben, N. 2020. An analysis of freeze–thaw cycles on geotechnical properties of soft-soil. Mater. Today: Proc. **27**: 1304–1309.

Qi, J., Vermeer, P.A., and Cheng, G. 2006. A review of the influence of freeze–thaw cycles on soil geotechnical properties. Permafr. Periglac. Process. **17**(3): 245–252. doi:10.1002/ppp.559.

Qin, Z.P., Lai, Y.M., Tian, Y., and Zhang, M.Y. 2021. Effect of freeze–thaw cycles on soil engineering properties of reservoir bank slopes at the northern foot of Tianshan Mountain. J. Mt. Sci. **18**(2): 541–557. doi: 10.1007/s11629-020-6215-z.

Tla, B., Cz, A., Ping, C.A., and Kz, A. 2020. Freeze–thaw damage evolution of fractured rock mass using nuclear magnetic resonance technology. Cold Reg. Sci. Technol. **170**: 102951.

Viklander, P. 1998. Permeability and volume changes in till due to cyclic freeze-thaw. Can. Geotech. J. **35**(3): 471–477. doi:10.1139/t98-015.

Wang, L.Q., Wang, Z.Q., Xin, F., Li, K.Y., Li, S., and Hu, X.Y. 2021. Strength and structure of Q_3 paleosol. Chin. J. Geotech. Eng. **43**(S1): 209–213.

Wang, W.N., Zhi, X.L., Mao, X.S., Hou, Z.J., and Lei, M.X. 2010. Experimental study of resilience modulus of subgrade soil under circles of freezing and thawing. J. Glaciol. Geocryol. **32**(5): 954–959.

Wu, Y.T., Ye, W.J., Yang, G.G., and Duan, Z. 2019. Experimental research on micro-pore and macro-deformation characteristics of soils considering stress paths. Chin. J. Rock Mech. Eng. **38**(11): 2311–2321.

Xu, J., Li, Y., Ren, C., Wang, S., and Chen, G. 2020. Influence of freeze-thaw cycles on microstructure and hydraulic conductivity of saline intact loess. Cold Reg. Sci. Technol. 181.

Ye, W.J., Wei, W. Zheng, C., et al. 2019a. Effect of initial moisture content on mechanical properties of expansive paleosol. J. Civ. Eng. Manage. **36**(4): 28–32.

Ye, W.J., Wu, Y.T. Yang, G.G., et al. 2019b. Study on microstructure and macro-mechanical properties of paleosol under dry–wet cycles. Chin. J. Rock Mech. Eng. **38**(10): 2126–2137.

Ye, W.J., Chen, Y.Q., Gao, C., Xie, T.F., and Deng, Y.S. 2021a. Experimental study on the microstructure and expansion characteristics of paleosol based on spectral scanning. J. Spectrosc. **2021**: 1–11.10.1155/2021/6689073.

Ye, W.J., Chen, Y.Q., Zhang, D.F., and Bai, Y. 2021b. Macro and micro experiment study on the influence of moisture migration on the strength of compacted loess under freeze–thaw cycling. Chin. J. Highw. Transp. **34**(06): 27–37.

Zhao, G.T., Han, Z, Zou, W.L., and Wang, X.Q. 2021. Influences of drying–wetting–freeze–thaw cycles on soil–water and shrinkage characteristics of expansive soil. Chin. J. Geotech. Eng. **43**(06): 1139–1146.

Zhang, W., Ma, J., and Tang, L. 2019. Experimental study on shear strength characteristics of sulfate saline soil in Ningxia region under long-term freeze–thaw cycles. Cold Reg. Sci. Technol. **160**: 48–57.

Zhang, Y., Bing, H., and Yang, C.S. 2015. Influence of freeze–thaw cycles on mechanical porperties of silty clay based on SEM and MIP test. Chin. J. Rock Mech. Eng. **34**(S1): 3597–3603.

Zhang, Z., Ma, W., and Qi, J.L. 2013. Strcture evolution and mechanism of engineering properties change of soils under effect of freeze–thaw cycle. J. Jilin Univ. (Earth Science Edition) **43**(6): 1904–1914.